

# Crystal Structure and Spectroscopic Study of Novel Two- and Three-Dimensional Photoluminescent Eu(III)–Adipate Compounds

YooJin Kim, Myungkoo Suh, and Duk-Young Jung\*

Department of Chemistry-BK21 and the Institute of Basic Sciences, Sungkyunkwan University, Suwon 440-746, Korea

Received April 21, 2003

Two new photoluminescent compounds with the formulas of  $[\text{Eu}_2(\text{adipate})_3(\text{H}_2\text{O})]\cdot\text{H}_2\text{O}$  (**1**) and  $[\text{Eu}_2(\text{adipate})_3(4\text{H}_2\text{O})]$  (**2**) were synthesized by using Eu(III) chloride and adipic acid under hydrothermal reaction conditions in aqueous solution. Compound **1**, a 3-D layered framework, possesses infinite Eu–O–Eu polyhedral chains and self-assembled adipate ligands between Eu–O layers. Compound **2** has dimeric  $\text{Eu}_2\text{O}_{16}$  units interconnected by adipate ligand, resulting in 2-D open frameworks with a cavity among the ligands. Crystal data **1**: monoclinic space group  $C2/c$ , with  $a = 14.2486(12)$  Å,  $b = 8.2733(7)$  Å,  $c = 39.298(2)$  Å,  $\beta = 99.530(6)^\circ$ , and  $Z = 8$ . **2**: monoclinic space group  $P2_1/c$ , with  $a = 11.661(4)$  Å,  $b = 14.011(3)$  Å,  $c = 9.013(4)$  Å,  $\beta = 110.87(3)^\circ$ , and  $Z = 2$ . The ligand conformations of two Eu(III)–adipate (**1** and **2**) compounds present anti/anti/anti, gauche/anti/gauche, and intermediate forms. Both compounds **1** and **2** showed strong red luminescence upon excitation, and their luminescence decay involves the multiphonon relaxation mechanism.

## Introduction

The synthesis of organic–inorganic hybrid open framework materials based on transition metals has become widespread over the past decade due to their magnetic properties,<sup>1</sup> ion exchanger,<sup>2</sup> precursors for oxides and catalysis.<sup>3</sup> Particularly, porous rare earth metal–organic compounds have interesting structures as well as potential application such as storage, gas sorption isotherms,<sup>4</sup> and optoelectronic.<sup>5</sup>

The increased activity in the field of metal carboxylates<sup>6</sup> is primarily due to the wide variety of structures that can be

introduced by the appropriate choice of organic moiety bound to the metal cation and reliable control of synthetic conditions. We have reported the crystal structure of transition metal–adipate compounds synthesized by hydrothermal method and found that the reaction parameters such as temperature, concentration, and pH are critical for successful synthesis.<sup>7</sup> The structure of these compounds can be characterized as a single layer of  $\text{MO}_6$  ( $M = \text{Mn}$  and  $\text{Fe}$ ) polyhedral chains separated by close packed crystalline alkyl chains, illustrating the possibility of synthesis of new layered metal dicarboxylates, by self-assembly from the molecular precursors.

The metal–dicarboxylate compounds of  $n > 4$  in  $-\text{O}_2\text{C}(\text{CH}_2)_n\text{CO}_2^-$ ,  $n = 0 - \infty$ , form layer like metal–oxygen networks,<sup>6a</sup> on the contrary, those of  $n$  smaller than 4 produce various multidimensional networks.<sup>8</sup> The structural variation is ascribed to not only the metal–oxygen coordination modes but also the ligand conformations to construct their 2D or

\* Author to whom correspondence should be addressed. E-mail: dyjung@chem.skku.ac.kr. Fax: 82-31-290-7075.

- (1) Gutschke, S. O. H.; Price, D. J.; Powell, A. K.; Wood, P. T. *Angew. Chem., Int. Ed.* **2001**, *40*, 1920.
- (2) (a) Yaghi, O. M.; Li, H. *J. Am. Chem. Soc.* **1996**, *118*, 295. (b) Robinson, F.; Zaworotko, M. J. *J. Chem. Soc., Chem. Commun.* **1995**, 2413.
- (3) (a) Seo, J. S.; Whang, D.; Lee, H.; Jun, S. I.; Oh, J.; Jeon, Y. J.; Kim, K. *Nature* **2000**, *404*, 982. (b) Kondo, M.; Okubo, T.; Asami, A.; Noro, S.; Yoshitomi, T.; Kitagawa, S.; Ishii, T.; Matsuzaka, H.; Seki, K. *Angew. Chem., Int. Ed.* **1999**, *38*, 140. (c) Eddaoudi, M.; Kim, J.; Rosi, N.; Vodak, D.; Wachter, J.; O'Keeffe, M.; Yaghi, O. M. *Science* **2002**, *295*, 469.
- (4) Reineke, T. M.; Eddaoudi, M.; O'Keeffe, M.; Yaghi, O. M. *Angew. Chem., Int. Ed.* **1999**, *38*, 2590.
- (5) (a) Lin, W.; Wang, Z.; Ma, L. *J. Am. Chem. Soc.* **1999**, *121*, 11249. (b) Evans, O. R.; Xiong, R.; Wong, G. K.; Lin, W. *Angew. Chem., Int. Ed.* **1999**, *38*, 536. (c) Reineke, T. M.; Eddaoudi, M.; Fehr, M.; Kelley, D.; Yaghi, O. M. *J. Am. Chem. Soc.* **1999**, *121*, 1651.

- (6) (a) Kim, Y. J.; Lee, E. W.; Jung, D. Y. *Chem. Mater.* **2001**, *13*, 2684. (b) Huang, Z.-L.; Drillon, M.; Masciocchi, N.; Sironi, A.; Zhao, J.-T.; Rabu, P.; Panissod, P. *Chem. Mater.* **2000**, *12*, 2805. (c) Serpaggi, F.; Férey, G. *Microporous Mesoporous Mater.* **1999**, *32*, 311. (d) Serpaggi, F.; Férey, G. *J. Mater. Chem.* **1998**, *8*, 2737.
- (7) (a) Kim, Y. J.; Jung, D. Y. *Inorg. Chem.* **2000**, *39*, 1470. (b) Kim, Y. J.; Jung, D. Y. *Bull. Korean Chem. Soc.* **2000**, *21*, 656.
- (8) (a) Forster, P. M.; Cheetham, A. K. *Angew. Chem., Int. Ed.* **2002**, *41*, 457. (b) Livage, C.; Egger, C.; Férey, G. *Chem. Mater.* **2001**, *13*, 410. (c) Lee, E. W.; Kim, Y. J.; Jung, D. Y. *Inorg. Chem.* **2002**, *41*, 501.

3D structures. The conformational isomerism of ligands has driven much interest in crystal engineering.<sup>9</sup> For example, cis and trans conformations of 1,4-cyclohexanedicarboxylates (chdc) are ascribed to construction of different structures of the final La–dicarboxylate compounds.<sup>10</sup> In the aliphatic dicarboxylate ligands, adipate ligand has a medium size carbon chain between terminal carboxylate groups, which invokes similar choice of flexible conformations as the chdc ligand. Thus, the appropriate combination of ligands and metals would develop various multidimensional systems. The reported adipate complexes of manganese(II),<sup>7a</sup> iron(II),<sup>7b</sup> zinc(II),<sup>11</sup> copper(II),<sup>12</sup> and lanthanum(III)<sup>13</sup> contain different structures and coordination modes. A guiding principle of our work is the attempt to understand the conformational variation of flexible spacer ligands in the architecture of the products.

The open frameworks of lanthanide dicarboxylate compounds also give us valuable information on correlation between the structure and photoluminescence property of rare earth–oxygen polyhedra. Especially, hydrothermal reaction enhances metal–ligand interactions rather than metal–water coordination, and finally this method could produce three-dimensional networks as clearly demonstrated in several dicarboxylate compounds.<sup>8</sup> The products prepared by hydrothermal reaction generally present relatively compact crystal structures and reduce metal–aqua coordination geometry to induce condensed metal–oxygen frameworks.

Herein we report the syntheses and luminescent properties of two new Eu–adipate compounds, [Eu<sub>2</sub>(adipate)<sub>3</sub>(H<sub>2</sub>O)](H<sub>2</sub>O) (**1**) and Eu<sub>2</sub>(adipate)<sub>3</sub>(4H<sub>2</sub>O) (**2**) prepared by hydrothermal reaction in the pH controlled aqueous solution. These compounds have been characterized by FT-IR, microanalysis, thermal analysis, powder and single-crystal X-ray diffraction, and photoluminescence spectroscopy.

## Experimental Section

**Materials and Methods.** Europium chloride hexahydrate (99%), adipic acid (99%), and potassium hydroxide (99.99%) were used as received from Aldrich. A mixture of 0.37 g (1 mmol) of EuCl<sub>3</sub>·7H<sub>2</sub>O, 0.14 g (1 mmol) of adipic acid, and 2.0 mL (1 mmol) of 1 M KOH with a EuCl<sub>3</sub>:adipic acid:KOH molar ratio of 1:1:2 (pH = 7.0) was heated along with 5 mL of water in a 23 mL capacity Teflon-lined reaction vessel at 180 °C for 24 h and then cooled to room temperature by quenching in a cold water bath. The colorless crystals were collected by filtration, washed with distilled water, and dried at room temperature. The crystals were insoluble in water and stable in ambient conditions. A mixture of rectangular-shape crystals (**1**) and needlelike crystals (**2**) was obtained, and each phase could be manually separated. The yields were ca. 20% (**1**) and 15%

(**2**), respectively, based on the utilized europium. Elemental analyses were performed with the crystals, for **1**: Anal. Calcd (%): C, 28.0; H, 3.6. Found (%): C, 28.3; H, 3.7. For **2**: Anal. Calcd (%): C, 26.7; H, 4.0. Found (%): C, 26.8; H, 4.0.

Powder X-ray diffraction was performed on a MAC SCIENCE 18XMF diffractometer with Cu K $\alpha$  radiation, and the purity of each sample was confirmed by comparing with the hypothetical diffraction spectra based on the single-crystal data. Thermogravimetric analyses (TGA) were conducted on a TA Instruments SDT 2960. The samples were placed in platinum containers, and the data were recorded under a nitrogen atmosphere (heating rate of 10 °C/min from room temperature to 1000 °C). Infrared (IR) spectra were obtained in the 4000–500 cm<sup>-1</sup> range using a Nicolet 1700 FT-IR spectrometer. The samples were ground with dry KBr and pressed into a transparent disk. The synthesized compounds were transferred to quartz tubes, and the emission spectra of the solid samples were acquired by using an Aminco Bowmann series 2 spectrofluorometer equipped with a 7 W pulsed Xe lamp. For emission spectra, the samples were excited with 320 nm light and the luminescence was collected for 2 ms after 30  $\mu$ s delay in order to reduce the scattering excitation light. The time profile of the luminescence decay was measured by monitoring the 618 nm emission band from europium ions. Except the measurements at 77 K, all spectra were obtained at ambient temperature.

**Single-Crystal X-ray Diffraction.** Single-crystal X-ray data were collected on a Siemens P4 automated four-circle diffractometer equipped with graphite monochromated Mo K $\alpha$  radiation ( $\lambda$  = 0.71079 Å). Intensity data were corrected for absorption with  $\psi$ -scan data. All calculations were carried out with use of the SHELXTL programs. The structures of **1** and **2** are solved by direct methods (SHELX-86) and the standard difference Fourier techniques (SHELX-97).<sup>14</sup> All non-hydrogen atoms were refined anisotropically. All hydrogen atoms were calculated at idealized positions. The hydrogen on coordinated water molecule was refined separately according to electron density difference, but those of noncoordinated water were not refined.

A crystal of **1** with approximate dimensions 0.32 × 0.28 × 0.15 mm<sup>3</sup> was used. The unit-cell parameters suggested a monoclinic unit cell with two possible space groups C2/c and Cc. A statistical analysis of reflection intensities suggested a centrosymmetric space group, and the structure analysis converged in C2/c (No. 15). A crystal of **2** with 0.40 × 0.08 × 0.04 mm<sup>3</sup> was used. **2** belongs to the monoclinic system and was solved in the centrosymmetric space group P2<sub>1</sub>/c (No. 14). The summary of crystal data for **1** and **2** is presented in Table 1. Selected bond lengths and bond angles are given in Table 2.

## Results and Discussion

**Structural Analyses.** Eu(III) ions in **1** have two different coordination environments, one in eight and the other in nine oxygen atoms as shown in Figure 1. The Eu(1) site is linked to six adipate ligands and one oxygen from coordinated water molecule. Eu(2) coordinates to eight oxygen atoms only from the six adipate ligands. There are two types of Eu–oxygen bridging modes in **1**, as shown in Figure 2, the *anti-anti* and the *syn-anti* mode, similar to those of other La–carboxylate compounds.<sup>10</sup> The average Eu(1)–O bond distance of Eu–(1)O<sub>8</sub>(H<sub>2</sub>O) polyhedra gives 2.48 Å, and the largest Eu–

(9) (a) Moulton, B.; Zaworotko, M. J. *Chem. Rev.* **2001**, *101*, 1629. (b) Hennigar, T. L.; MacQuarrie, D. C.; Losier, P.; Rogers, R. D.; Zaworotko, M. J. *Angew. Chem., Int. Ed.* **1997**, *36*, 972. (c) Fujita, M.; Kwon, Y. J.; Miyazawa, M.; Ogura, K. *J. Chem. Soc., Chem. Commun.* **1994**, 1977.

(10) Kim, Y. J.; Jung, D. Y. *Chem. Commun.* **2002**, 908.

(11) Cai, J.; Long, L.-S.; Zheng, L.-S. *Main Group Met. Chem.* **2002**, *25*, 517.

(12) Forster, P. M.; Thomas, P. M.; Cheetham, A. K. *Chem. Mater.* **2002**, *14*, 17.

(13) Kiritsis, V.; Michaelides, A.; Skoulika, S.; Golhen, S.; Ouahab, L. *Inorg. Chem.* **1998**, *37*, 3407.

(14) McArdle, P. SHELX-86 and SHELX-97 Users Guide: Crystallography Center, Chemistry Department, National University of Ireland: Galway, Ireland; *J. Appl. Crystallogr.* **1995**, *28*, 65.

**Table 1.** Crystal Data and Structure Refinement for **1** and **2**

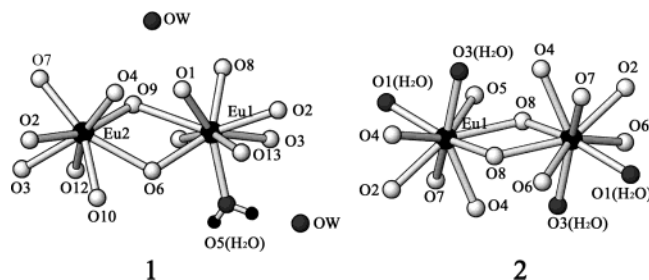
	<b>1</b>	<b>2</b>
formula	C <sub>18</sub> H <sub>28</sub> Eu <sub>2</sub> O <sub>14</sub>	C <sub>18</sub> H <sub>32</sub> Eu <sub>2</sub> O <sub>16</sub>
fw	772.34	808.39
crystal system	monoclinic	monoclinic
space group	C2/c (No. 15)	P2 <sub>1</sub> /n (No.14)
T (K)	296(2)	296(2)
a (Å)	14.2486(12)	11.661(4)
b (Å)	8.2737(7)	14.011(3)
c (Å)	39.298(2)	9.013(4)
β (deg)	99.530(6)	110.87(3)
V (Å <sup>3</sup> )	4568.7(6)	1375.9(8)
Z	8	2
D <sub>calcd</sub> (mg cm <sup>-3</sup> )	2.240	1.932
abs coeff (mm <sup>-1</sup> )	5.512	4.585
no. of reflns collected	4117	2566
no. of unique data	3947	2401
goodness-of-fit on F <sup>2</sup>	1.073	1.056
final R <sub>1</sub> <sup>a</sup>	0.0654	0.0480
final wR <sub>2</sub> <sup>b</sup>	0.1656	0.1137

<sup>a</sup> R<sub>1</sub> =  $\sum ||F_o| - |F_c|| / \sum |F_o|$ . <sup>b</sup> wR<sub>2</sub> =  $[\sum |w(F_o^2 - F_c^2)| / \sum w(F_o^2)]^{1/2}$ ,  $w = [\sigma(F)]^{-1}$ .

**Table 2.** Selected Bond Lengths (Å) for **1**<sup>a</sup> and **2**<sup>b</sup>

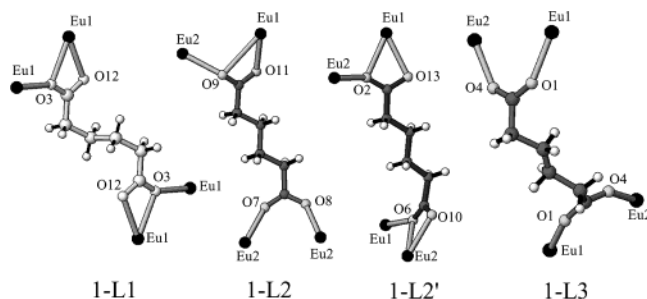
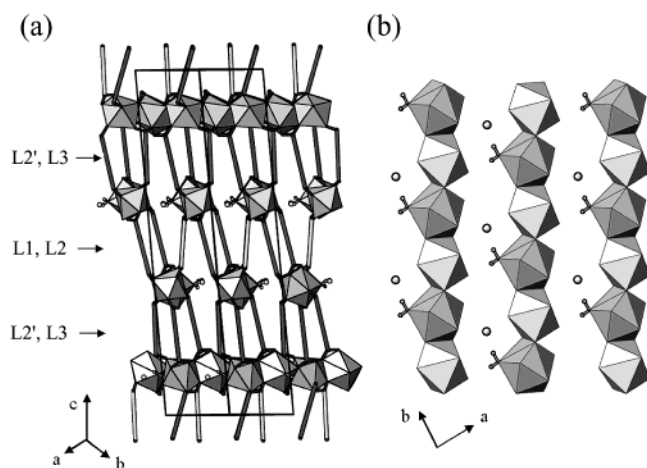
<b>1</b>		<b>2</b>	
Eu(1)–O(1)	2.348(10)	Eu(2)–O(4)	2.286(11)
Eu(1)–O(8)	2.360(10)	Eu(2)–O(7)	2.352(10)
Eu(1)–O(6)	2.401(11)	Eu(2)–O(9)	2.369(11)
Eu(1)–O(5)	2.422(13)	Eu(2)–O(2)	2.412(9)
Eu(1)–O(3)	2.428(9)	Eu(2)–O(10)	2.450(10)
Eu(1)–O(11)	2.433(9)	Eu(2)–O(12)	2.461(10)
Eu(1)–O(13)	2.506(10)	Eu(2)–O(3)	2.477(10)
Eu(1)–O(2)	2.516(9)	Eu(2)–O(6)#2	2.586(10)
Eu(1)–O(9)#1	2.920(12)		
		Eu(1)–O(1)	2.389(8)
		Eu(1)–O(3)	2.399(7)
		Eu(1)–O(8)#1	2.411(7)
		Eu(1)–O(2)	2.426(8)
		Eu(1)–O(4)	2.469(7)
		Eu(1)–O(7)	2.503(8)
		Eu(1)–O(5)	2.503(7)
		Eu(1)–O(6)	2.514(8)
		Eu(1)–O(8)	2.558(7)

<sup>a</sup> Symmetry transformations used to generate equivalent atoms for **1**: #1  $x + 1/2, y + 1/2, z$ ; #2  $x - 1/2, y - 1/2, z$ ; #3  $-x + 1, -y, -z + 1$ ; #4  $-x + 3/2, -y - 1/2, -z + 1$ ; #5  $-x + 1, y, -z + 3/2$ . <sup>b</sup> Symmetry transformations used to generate equivalent atoms for **2**: #1  $-x, -y, -z$ ; #2  $x - 1, y, z$ ; #3  $x + 1, y, z$ ; #4  $-x + 1, -y, -z + 1$ .

**Figure 1.** The coordination environments of the Eu(III)–O polyhedra in **1** (left) and **2** (right).

O(9) of 2.92 Å results from edge-sharing Eu–O bond. Also, the distances of Eu(2)–O vary in the range of 2.286 to 2.586 Å, which consist of three short (2.286–2.369 Å) and five long ones (2.412–2.586 Å). The solvate water molecule (OW) has hydrogen bonding<sup>15</sup> with O5 (coordinated water), with a O(5)–H···O(W) distance of 2.5 Å and angle of 143.7°. This hydrogen bonding between solvate water and the carboxylate oxygen is observed in many other cases.<sup>16</sup> The two oxygen atoms from the water and the carboxylate group are also close enough for hydrogen bonding (OW–O8 at 2.80 Å and OW–O8 at 2.86 Å, OW–O9 at 2.92 Å,

(15) Braga, D.; Grepioni, F.; Desiraju, G. R. *Chem. Rev.* **1998**, *98*, 1375.  
 (16) Kim, Y. J.; Jung, D. Y. *Inorg. Chim. Acta* **2002**, *338*, 229.

**Figure 2.** Four ligand conformations, 1-L1 (gauche/anti/gauche), 1-L2 (anti/anti/anti), 1-L2' (anti/anti/anti), and one 1-L3 (intermediate) are observed in **1**.**Figure 3.** Perspective view of **1** down the [111] direction (a) and polyhedral view in a direction approximately parallel to the [100] direction (b).

OW–O1 at 3.08 Å), but placing a hydrogen atom of water molecule along these vectors leads to unreasonable geometries.

The Eu(1)O<sub>9</sub> and Eu(2)O<sub>8</sub> polyhedra are edge-shared through O9 and O6, which create one-dimensional infinite chains as schematized in Figure 3. It should be noted that the Eu(III) chain structure is a unique model system for studying the artificial one-dimensional infinite europium(III)–oxide. The complex connection of compound **1** involves the formation of Eu–O layer with alkyl chains assembled along [001] direction. These edge shared Eu–O chains are parallel to the *ab* plane in the unit cell and form infinite Eu–O layers between adipate ligands similar with the Mn/Fe–adipate compound.<sup>7</sup> A unit cell of **1** involves four Eu–O layers, of which two layers in a row are assembled along the *b*-axis and next two other layers along the *a*-axis, as shown in Figure 3. This alternating of directions of Eu–O layers contrasts with the unidirectional MnO<sub>6</sub> ribbon chains in Mn–adipate compounds<sup>7</sup> where zigzag layers arrange parallel to a unique direction.

The organic and inorganic layers of **1** are stacked along the *c*-axis, and the interlayer spacing is 9.68 Å. The hydrophobic characteristic of alkyl chains induces self-assembly of organic moiety leading to the complete packing of interlayer spaces. There are four crystallographically independent adipate ligands in **1**, and they are represented as 1-L1 (gauche/anti/gauche), 1-L2 (anti/anti/anti), 1-L2' (anti/anti/anti), and 1-L3 (intermediate) in Figure 2. Their

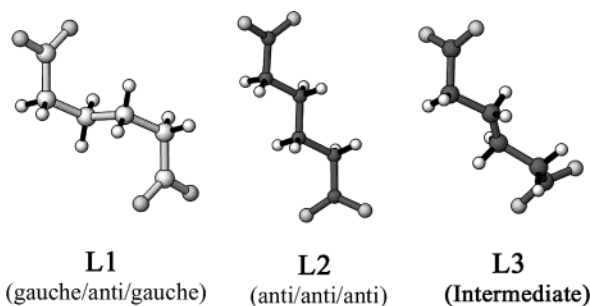


**Figure 4.** Three representative conformations of adipate ligands in the present study, L1 (gauche/anti/gauche), L2 (anti/anti/anti), and L3 (intermediate) adipate ligands.

**Table 3.** Angles (deg) of Carbon Chains for **1** and **2**<sup>a</sup>

compound	ligand	C <sub>a</sub> –C <sub>b</sub> –C <sub>c</sub>	C <sub>b</sub> –C <sub>c</sub> –C <sub>d</sub>	C <sub>c</sub> –C <sub>d</sub> –C <sub>e</sub>	C <sub>d</sub> –C <sub>e</sub> –C <sub>f</sub>
<b>1</b>	1-L1	115.9(14)	109.1(17)	109.1(17)	115.9(14)
	1-L2	111.7(12)	113.8(13)	114.8(14)	116.5(13)
	1-L2'	118.7(13)	110.9(12)	115.4(12)	109.2(12)
	1-L3	110.3(22)	130.8(33)	130.8(33)	110.3(22)
<b>2</b>	2-L1'	111.2(11)	145.6(29)	145.6(29)	111.2(11)
	2-L2''	111.5(9)	110.2(10)	116.0(11)	114.0(10)
adipic acid <sup>b</sup>		115.0	112.7	112.7	115.0
adipate ligand <sup>c</sup>		110.0	112.4	112.6	115.9
adipate ligand <sup>d</sup>		116.2	112.3	112.5	111.1

<sup>a</sup> The carbon atoms in adipate ligand are labeled as follows: adipate = [O<sub>2</sub>–C<sub>a</sub>–C<sub>b</sub>–C<sub>c</sub>–C<sub>d</sub>–C<sub>e</sub>–C<sub>f</sub>–O<sub>2</sub>]<sup>2-</sup>. <sup>b</sup> Reference 17. <sup>c</sup> Reference 7a. <sup>d</sup> Reference 7b.

**Table 4.** Torsion Angles (deg) of **1** and **2**<sup>a</sup>

compound	ligand	C <sub>a</sub> –C <sub>d</sub>	C <sub>b</sub> –C <sub>e</sub>	C <sub>c</sub> –C <sub>f</sub>
<b>1</b>	1-L1	70.5	180	70
	1-L2	174	178.5	169
	1-L2'	173	179	175
	1-L3	139	167	139
<b>2</b>	2-L1'	20	180	20
	2-L2''	168	174	174
adipic acid <sup>b</sup>		174	180	174
adipate ligand <sup>c</sup>		175	179	175
adipate ligand <sup>d</sup>		175	178	168

<sup>a</sup> The carbon atoms in adipate ligand are labeled as follows: adipate = [O<sub>2</sub>–C<sub>a</sub>–C<sub>b</sub>–C<sub>c</sub>–C<sub>d</sub>–C<sub>e</sub>–C<sub>f</sub>–O<sub>2</sub>]<sup>2-</sup>. <sup>b</sup> Reference 17. <sup>c</sup> Reference 7a. <sup>d</sup> Reference 7b.

compositional ratio in the crystal is 1:2:2:1. Each conformation could be assigned to three different isomers such as L1 (gauche/anti/gauche), L2 (anti/anti/anti), and L3 (intermediate), as schematized in Figure 4. The C–C–C bond angles and torsion angles are listed in Table 3 and Table 4. In particular, the angle values of anti/anti/anti ligands (1-L2 and 1-L2') are close to those of the reported adipic acid crystal structure<sup>17</sup> and also close to other adipate ligands of previous results.<sup>7</sup> All adipate ligands are located along the *c*-axis and surrounded by the six other ligands with a shorter interchain separation of about 4.3 Å, a value smaller than the chain–chain spacing observed in diacid (5.1 Å).<sup>17</sup> **1** has two types of ligand layers located between the parallel and perpendicular Eu–O chains. The 1-L1 and 1-L2 layers are bound between neighboring Eu–O layers with parallel Eu–O chains, however, their upper and lower layers, 1-L2' and 1-L3, involve those with perpendicular Eu–O chains. In the former layers, 1-L1 is surrounded by six 1-L2, but 1-L2 by

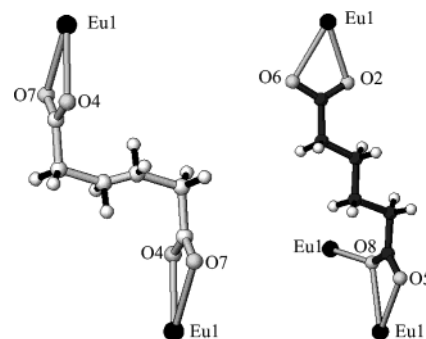


**Figure 5.** Two ligand conformations, 2-L1' (gauche/anti/gauche) and 2-L2'' (anti/anti/anti), are observed in **2**.

three 1-L1 and three 1-L2 ligands. In the latter case, 1-L3 is surrounded by six 1-L2', but 1-L2' by three 1-L3 and three 1-L2' ligands. The regular array of isomeric alkyl chains is ascribed to self-assembly of flexible adipate ligands as well as the infinite edge-shared Eu(III)–O coordination network.

The crystal structure of **2** consists of nine oxygen atoms coordinated to Eu(III), as shown in Figure 1, of which seven oxygen atoms come from four adipate (one 2-L1 and three 2-L2'') ligands and two from the two independent coordinated water molecules. The Eu–O bond distances range from 2.389(8) to 2.558(7) Å. Two symmetric EuO<sub>9</sub> polyhedra share their edges to form a Eu<sub>2</sub>O<sub>16</sub> dimeric unit which has an inversion center between two Eu(III) ions. There are two types of Eu–oxygen bridging modes in **2**, the *syn-syn* and the *syn-anti* mode as shown in Figure 5. The previous La–adipate<sup>13</sup> prepared in ambient conditions consists of three kinds of bridging modes (*syn-syn*, *syn-anti*, *anti-anti*) and infinite dimer units running along a unique one-direction. The connection between infinite dimer units and adipate ligand is responsible for the formation of relatively large infinite channels in the La–adipate compound. The coordination mode of each carboxylate ligand provides important information predicting the topology of the resulting network,<sup>18</sup> and therefore, rare earth metal–carboxylate compounds are more useful than transition metal–carboxylate for studying metal–carboxylate bridging modes owing to large ionic radii of lanthanide elements. A Eu<sub>2</sub>O<sub>16</sub> dimer is connected to four neighboring other Eu<sub>2</sub>O<sub>16</sub> units through coordination with six adipate ligands and two 2-L1' (gauche/anti/gauche) ligands along the [101] direction, and four 2-L2'' (anti/anti/anti) ligands along the [100] direction. The ratio of 2-L1' to 2-L2'' is 1:2, and the L3 type ligands observed in **1** are absent in **2**. The topology creates lozenge-shaped nets made from four edge-shared Eu<sub>2</sub>O<sub>16</sub> and six adipate ligands, which produces small cavity as shown in Figure 6. This arrangement generates extended sheets along the (010) plane. The resulting infinite two-dimensional networks are stacked along the *b*-axis as shown in Figure 7.

It is worth comparing the crystal structures of **1** and **2** with the previously reported 3D open-frameworks of rare earth metal–adipate compounds which were synthesized in

(17) Thalladi, V. R.; Nüsse, M.; Boese, R. *J. Am. Chem. Soc.* **2000**, *122*, 9227.

(18) Eddaoudi, M.; Moler, D. B.; Li, H.; Chen, B.; Reineke, T. M.; O'Keeffe, M.; Yaghi, O. M. *Acc. Chem. Res.* **2001**, *34*, 319.

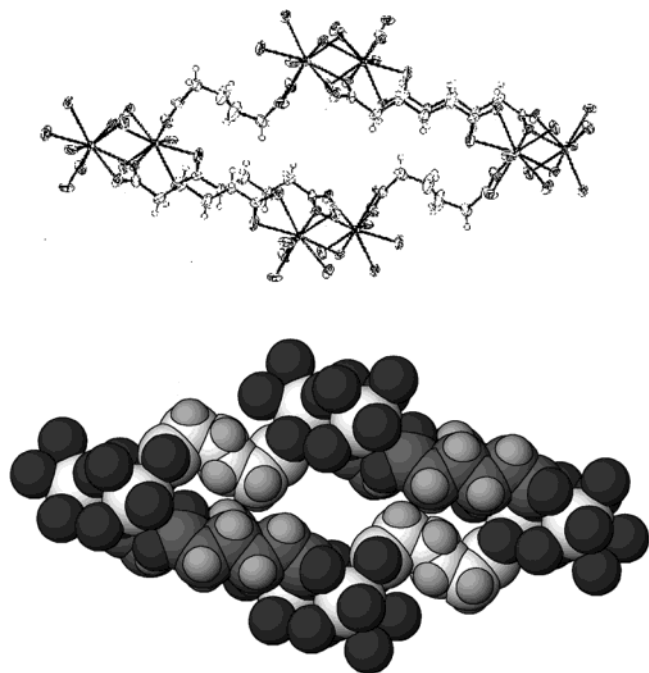


**Figure 6.** The lozenge-shaped nets made from  $\text{Eu}_2\text{O}_{16}$  and adipate ligands in **2**.

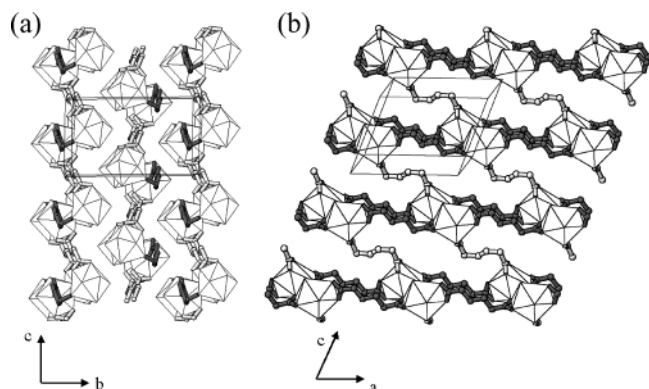


**Figure 7.** Representation of the extended structure of **2**. (a) View down [100] of stacking and (b) view down [010] of network of one sheet.

gel–solution methods at ambient temperature.<sup>13,19</sup> First, the compounds prepared in ambient conditions reveal that the total numbers of water molecules are critical to determine structural topologies such as interpenetration.<sup>19,20</sup> On the contrary, we could prepare more dense frameworks than those in the previous compounds,<sup>13</sup> because the hydrothermal reactions have a reduced metal–water coordination. Second, the structure of **2** invokes 2-D noninterpenetrated open framework, related with hydrothermal syntheses driving the compact organic–inorganic network. In general, the two or three folded interpenetrating open frameworks occupy only a small fraction of the available space in the crystal. Third, each compound consists of different ratios of the conformational isomers of adipate ligands. To measure the confor-

(19) (a) Dimos, A.; Tsaousis, D.; Michaelides, A.; Skoulika, S.; Golhen, S.; Ouahab, L.; Didierjean, C.; Aubry, A. *Chem. Mater.* **2002**, *14*, 2616. (b) Sun, Z.-G.; Ren, Y.-P.; Long, L.-S.; Huang, R.-B.; Zheng, L.-S. *Inorg. Chem. Commun.* **2002**, *5*, 629.

(20) Yaghi, O. M.; Li, H. *J. Am. Chem. Soc.* **1996**, *118*, 295.

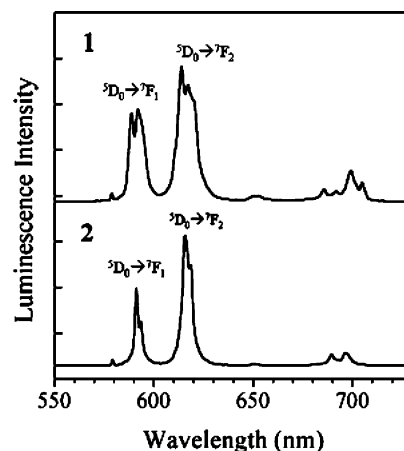


**Figure 8.** Photoluminescence spectra of **1** and **2**. The excitation wavelength was 320 nm, and spectra are taken at ambient temperature.

mational torsion of our products, the angles of carbon chains are summarized in Table 3. It should be noted that the final refined structural data show large anisotropic thermal factors for the middle carbons of 1-L3 ligands, demonstrating the flexibility of the 1-L3 chains in the framework. When metal–carboxylate compounds were constructed, gauche forms were shown in crystal assembled although the energy of anti forms was favored.

**Thermal Analyses.** TGA studies of **1** and **2** were carried out in a nitrogen atmosphere from room temperature to 1000 °C with a heating rate of 10 °C/min. Two major weight losses of compound **1** occurred at 110–200 °C and 320–350 °C. TGA of **1** displays that the first weight loss of the water molecules (two noncoordinated water and two coordinated water) started at about 110 °C and completed at 200 °C (obsd 7.8%, calcd 7.6%). Distinction between weight losses from the coordinated and noncoordinated water was not clearly demonstrated in TGA data. This nondistinctive behavior is also reported in  $[\text{La}_2(\text{cis-chdc})_2(\text{trans-chdc})(2\text{H}_2\text{O})](2\text{H}_2\text{O})$ ,<sup>10</sup> which consists of coordinated and noncoordinated water. For **2**, the TGA curve was very similar to the result of **1** and the compound was stable up to 330 °C. The release of coordinated water occurred between 90 and 170 °C (obsd 9.2% calcd 8.9%). The 48% mass loss (310–600 °C) corresponds to the decomposition of the organic chains through the pyrolysis reaction. The resulting products after the TG analysis have  $\text{Eu}_2\text{O}_3$  phase characterized by the powder X-ray diffraction spectra.

**Photoluminescence Measurements.** The compounds **1** and **2** emitted strong red luminescence upon excitation with 320 nm, and their photoluminescence spectra are depicted in Figure 8. The transitions  $^5\text{D}_0 \rightarrow ^7\text{F}_n$  ( $n = 0-4$ ) of **1** appeared as emission bands at 580, 590, 618, 652, and 695 nm, respectively. Overall, the luminescence spectra of the two samples are similar except that the bands of **1** are broader than those of **2**, indicating that the coordination environment of **1** is more inhomogeneous than that of **2**. It is noted that the intensity of the hypersensitive transition  $^5\text{D}_0 \rightarrow ^7\text{F}_2$  is comparable to that of  $^5\text{D}_0 \rightarrow ^7\text{F}_1$ . Since the former transition is electric dipole in nature, its intensity is strongly influenced by the crystal field while the latter transition is magnetic

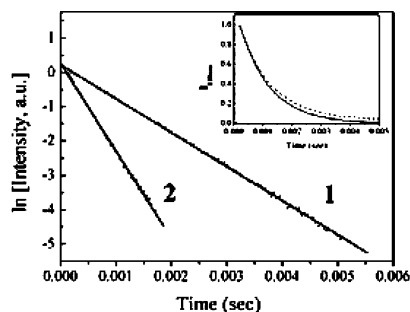


**Figure 9.** Luminescence decay curves for **1** and **2** at ambient temperature. The solid lines are the best fits of experimental data. The inset compares decay curves of **1** at ambient temperature (solid line) and at 77 K (dashed line).

dipole in origin and less sensitive to its environment.<sup>21</sup> The comparable intensities of  ${}^5D_0 \rightarrow {}^7F_1$  and  ${}^5D_0 \rightarrow {}^7F_2$  transitions imply relatively symmetric crystal fields for both **1** and **2**.<sup>22</sup> The luminescence spectra at 77 K for the prepared compounds present similar relative intensities and narrower emission lines, compared to those obtained at room temperature.

Unlike the similarity of photoluminescence spectra, luminescence lifetimes of **1** and **2** are quite different as shown in Figure 9. The experimental curves fit well with single exponential decays of which the lifetime is 1.0 ms for **1** and 0.38 ms for **2**, respectively. Vibrations of water molecules can effectively remove the electronic energy of excited europium ions, and the extent of the quenching is directly related to the number of coordinated water molecules.<sup>23</sup> The hydration number ( $n$ ) in crystalline Eu(III) complexes can be estimated from the lifetime,  $\tau$  in ms, by using the equation  $n = 1.05\tau^{-1} - 0.70$ .<sup>24</sup> The hydration number of **2** was calculated to be 2.1, which is in good agreement with the structural data where four water molecules are coordinated to isolated dimeric  $\text{Eu}_2\text{O}_{12}(\text{H}_2\text{O})_4$  as shown in Figure 1.

On the other hand, compound **1** exhibited a single luminescence lifetime of 1.0 ms, corresponding to 0.35 molecule per Eu(III) despite the fact that **1** has two distinct Eu sites [ $\text{Eu}(1)\text{O}_8(\text{H}_2\text{O})$  and  $\text{Eu}(2)\text{O}_8$ ]. It should be noted that Eu–O polyhedra form infinite one-dimensional Eu–O–Eu chains. In addition, solvate water molecules contribute hydrogen-bonding network between coordinated water and carboxylate oxygen atoms as shown Figure 3b. Therefore, the observed single luminescence lifetime is attributed to the effective coupling between Eu(1) and Eu(2) sites as well as extensive hydrogen bonding network. Previously, the participation of water molecules in outer coordination sphere

has been suggested to explain the fractional hydration number of Eu(III) complexes in solution.<sup>25</sup>

To investigate the origin of this complex relaxation, we measured the luminescence lifetime of **1** at 77 K. In this temperature region, multiphonon relaxation by coupling to O–H vibrations is essentially independent of the temperature, while energy transfer processes are strongly temperature dependent.<sup>26</sup> The luminescence decay of **1** at 77 K exhibited dual lifetimes; the predominant one with 90% contribution was 1.0 ms, identical to the value at room temperature, and a slower minor (10%) decay was 4.3 ms. This essentially temperature-independent characteristic of the lifetime proves that the single lifetime observed in **1** is mainly due to the multiphonon relaxation by coupling to O–H vibrations.

## Conclusion

This work demonstrates that two novel Eu(III)–adipate compounds with different ligand conformations have been crystallized simultaneously in hydrothermal reaction. The structure of **1** involves the novel feature that the anionic layer is assembled with Eu(III) cations and close-packed alkyl chains residing in an extended Eu–O polyhedral framework. High coordination numbers of Eu(III) and the flexibility of adipate ligands may help to adopt self-assembly of alkyl chains in **1**. Unlike transition metal dicarboxylates, the Eu–adipate system by hydrothermal synthesis also gave another structural type, compound **2**, a new two-dimensional structure which has isolated dimeric Eu–O polyhedral units. The formation of a coordination polymer containing rare earth metal cations may be driven by high stability constant with carboxylate ligands. The photoluminescence spectra and lifetimes of the prepared compounds were successfully explained according to the Eu–O coordination environments and hydrogen bonding networks.

**Acknowledgment.** We acknowledge support by the Electron Spin Science Center at POSTECH, which was established by the KOSEF. Y.K. thanks the Ministry of Education, Republic of Korea, for the scholarship through the Brain Korea 21 program.

**Supporting Information Available:** X-ray crystallographic files, in CIF format, for  $[\text{Eu}_2(\text{adipate})_3(\text{H}_2\text{O})] \cdot \text{H}_2\text{O}$  (**1**) and  $[\text{Eu}_2(\text{adipate})_3(4\text{H}_2\text{O})]$  (**2**). This material is available free of charge via the Internet at <http://pubs.acs.org>.

IC034418K

(21) Kirby, A. F.; Foster, D.; Richardson, F. S. *Chem. Phys. Lett.* **1983**, 95, 507.

(22) Bunzli, J.-C. G. In *Lanthanide Probes in Life, Chemical and Earth Sciences, Theory and Practice*; Bunzli, J.-C. G., Choppin, G. R., Eds.; Elsevier: New York, 1989; p 219.

(23) (a) Choppin, G. R.; Peterman, D. R. *Coord. Chem. Rev.* **1998**, 174, 283. (b) Choppin, G. R.; Peterman, D. R. *Coord. Chem. Rev.* **1998**, 174, 283. (c) Horrocks, W. de W., Jr.; Sudnick, D. R. *Acc. Chem. Res.* **1981**, 14, 384.

(24) Bartelmy, P. P.; Choppin, G. R. *Inorg. Chem.* **1989**, 28, 3354.

(25) Dickins, R. S.; Parker, D.; de Sousa, A. S.; Williams, J. A. G. *Chem. Commun.* **1996**, 697.

(26) (a) de Mello Donegá, C.; Ribeiro, S. J. L.; Gonçalves, R. R.; Blasse, G. *J. Phys. Chem. Solids*. **1996**, 57, 1727. (b) de Sá, G. F.; Malta, O. L.; de Mello Donegá, C.; Simas, A. M.; Longo, R. L.; Santa-Cruz, P. A.; da Silva, E. F., Jr. *Coord. Chem. Rev.* **2000**, 196, 165. (c) Serpaggi, F.; Luxbacher, T.; Cheetham, A. K.; Férey, G. *J. Solid State Chem.* **1999**, 145, 580. (d) Blasse, G.; Grabmaier, B. C. *Luminescent Materials*; Springer-Verlag: New York, 1994.